Computer simulations of colloidal dispersions

International Focus Workshop on

Novel Simulation Approaches to Soft Matter Systems

Dresden, September 20-24, 2010

by Hartmut Löwen

Heinrich-Heine-Universität Düsseldorf

Outline

1) Introduction
2) Colloidal sedimentation
3) Lane formation in driven colloids
4) Band formation in oscillatory fields
5) Lane formation in complex plasmas
6) Conclusions

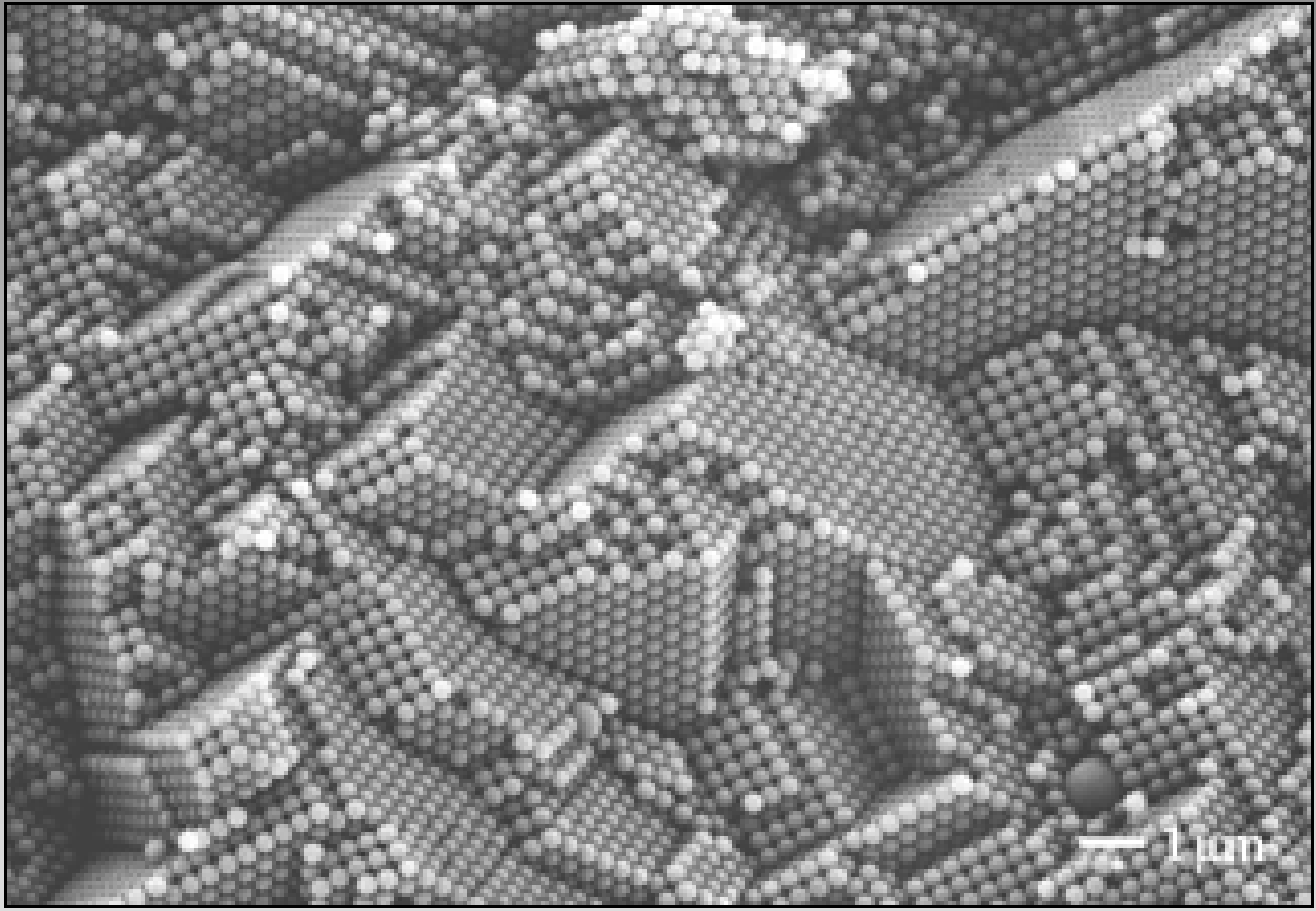

colloidal particles

(from A. Imhof and D. Pine)

Why colloidal dispersions?

- controlled preparation
- effective interaction can be **tailored**
- **complete separation** in length and time scales
- excellent **model systems**
- comparison

theory / computer simulation | experiment

→ - fundamental understanding
- explicit predictions

- colloids react **sensitively** upon external perturbations
- external field can induce **novel effects**
- external field can be **tailored**

→ **model driven systems**
under controlled non-bulk and
non-equilibrium conditions

Problem:
the colloidal dynamics involve solvent mediated hydrodynamic interactions!

among the possibilities to treat H.I.:

- neglect them! (ordinary BD)
- (long ranged) mobility tensors
- MPCD (multi-particle-collision dynamics)

see e.g.

Padding, Louis, PRE 74, 031402 (2006)

Gompper, Ihle, Kroll, Winkler, Adv. Polym. Science 221, 1 (2009)

- lattice Boltzmann (→ Ladd, Cates, Pagonabarraga,…)
- smoothed profile method (→ Yamamoto et al)
- fluid particle dynamics (→ Tanaka, Araki)

---

here: link to real-space experiments

Examples:

colloidal instabilities on the particle scale

- colloidal sedimentation
- lane formation in oppositely driven binary suspensions and dusty plasmas
- band-formation in oscillatory driven mixtures

recent review: HL, Soft Matter 6, 3133 (2010)

Collaborators:

Düsseldorf:	J. Dzubiella	M. Kohl
	M. Rex	A .Wysocki
Bristol:	P. Royall	
Utrecht:	A. van Blaaderen	T. Vissers
	A. Imhof	
Jülich:	G. Gompper	R. Winkler
Tokyo:	H. Tanaka	
Calkutta:	J. Chakrabrati	

Rayleigh-Taylor-like instability in the sedimentation of colloids

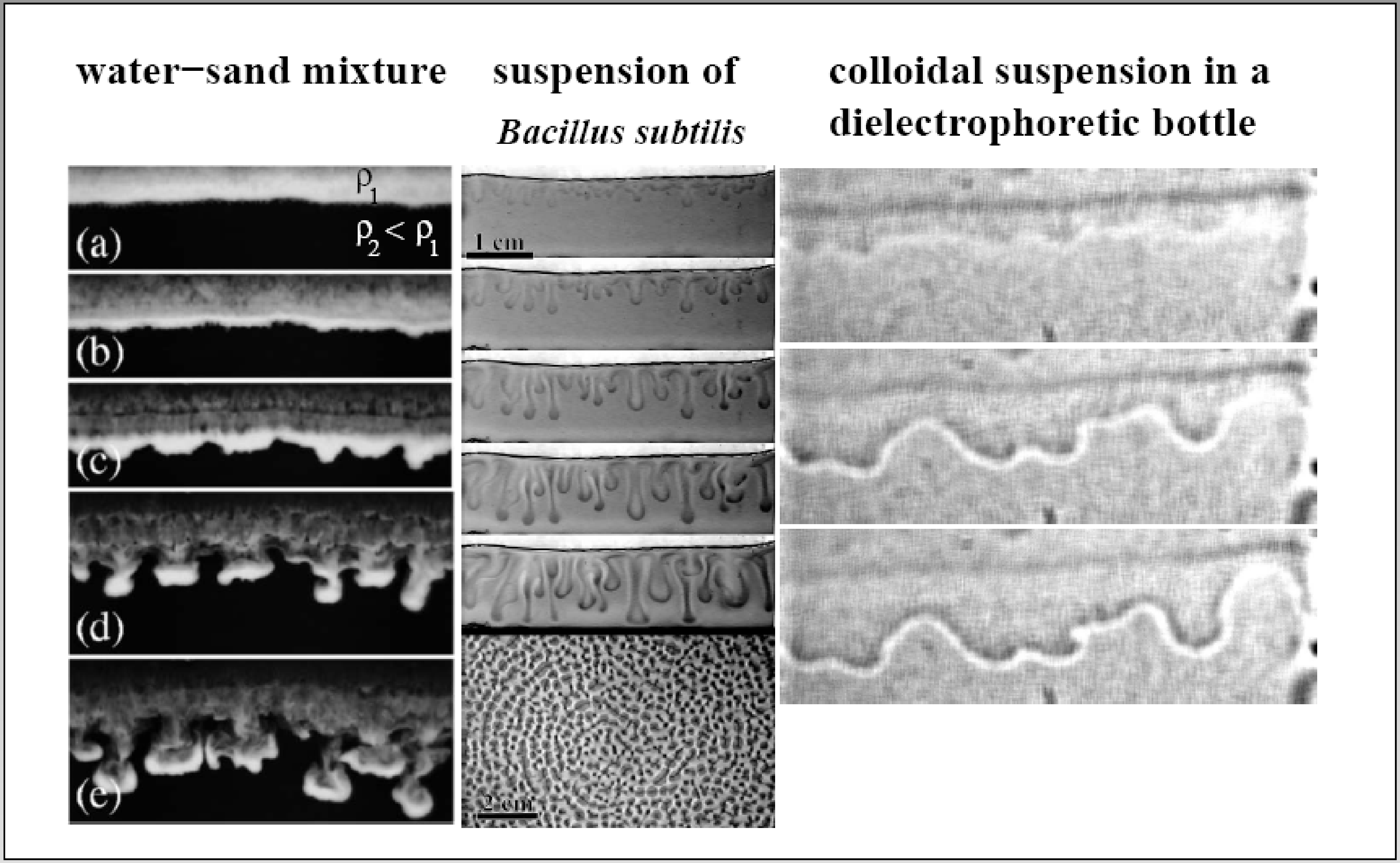

low Reynolds number

Peclet number $Pe = \frac{\tau_D}{\tau_S} = \frac{\text{convective transport}}{\text{diffusive transport}} = \frac{mg\sigma}{k_B T}$

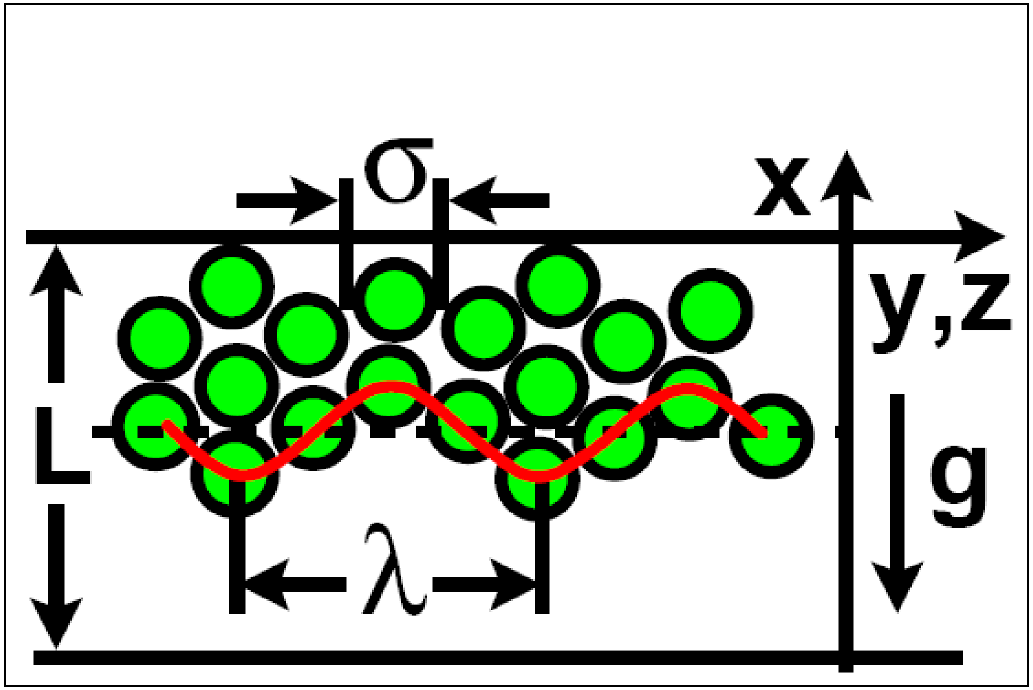

A. Wysocki, C.P. Royall, R.G. Winkler, G. Gompper, H. Tanaka, A. van Blaaderen, HL, Soft Matter 5, 1340 (2009)

Colloidal system (experiment)

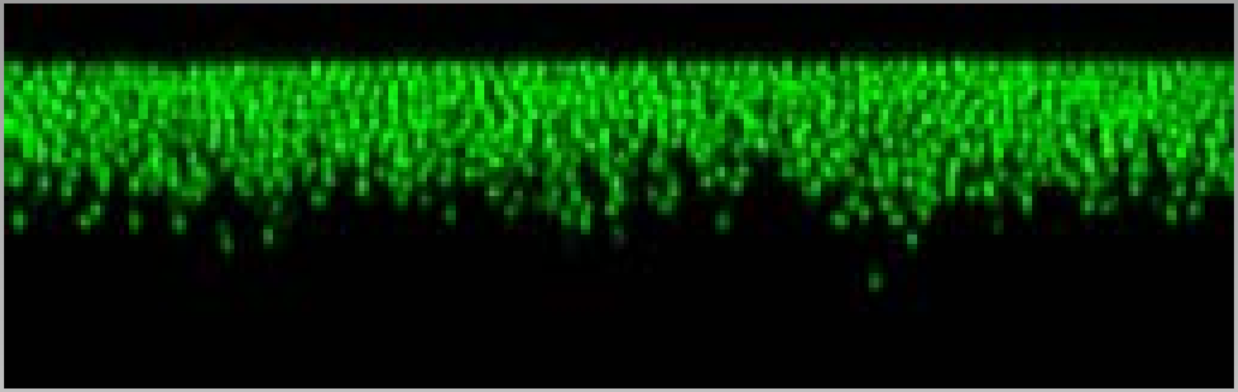

$Pe = 1.1$

$\frac{L}{\sigma} = 18$

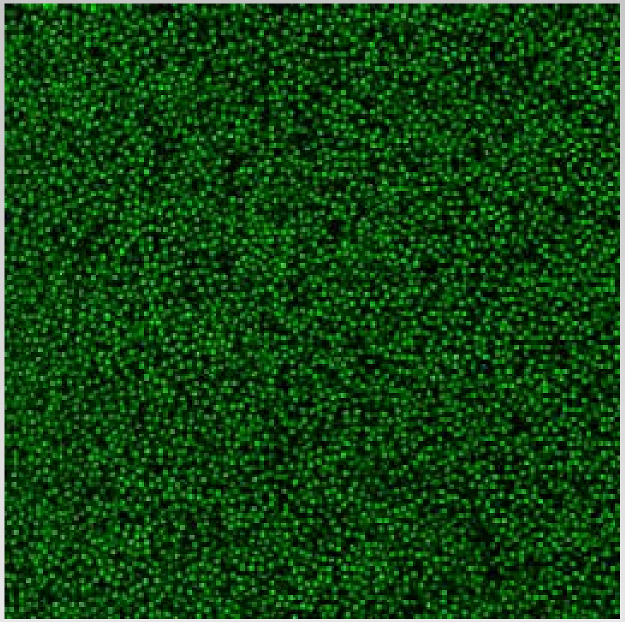

$\phi = 0.15$

MPCD, thechnical details

A. Wysocki, C.P. Royall, R.G. Winkler, G. Gompper, H. Tanaka, A. van Blaaderen, HL,

Faraday Discussions 144, 245 (2010)

$N = 15048$ "hard" spheres of diameter σ

$N_s = 14.200.000$ solvent particles

$L_y / \sigma = L_z / \sigma = 54 \qquad (L_x / \sigma = 18,$ slit width$)$

Verlet velocity algorithm (including angular velocities)

no-slip boundary conditions via stochastic reflection method at colloidal surface

(Padding, Wysocki, HL, Louis, JPCM 17, S3393 (2005))

plus filling with ghost particles

(Lamura, Gompper, Ihle, Kroll, EPL 56, 319 (2001))

local thermostat for solvent

$M = 167m$ colloidal mass

$\sigma = 4a$

Computer simulation

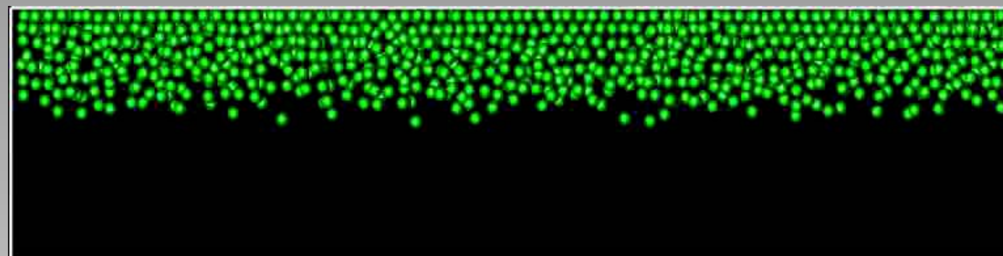

$$Pe = 1.1$$

$$\frac{L}{\sigma} = 18$$

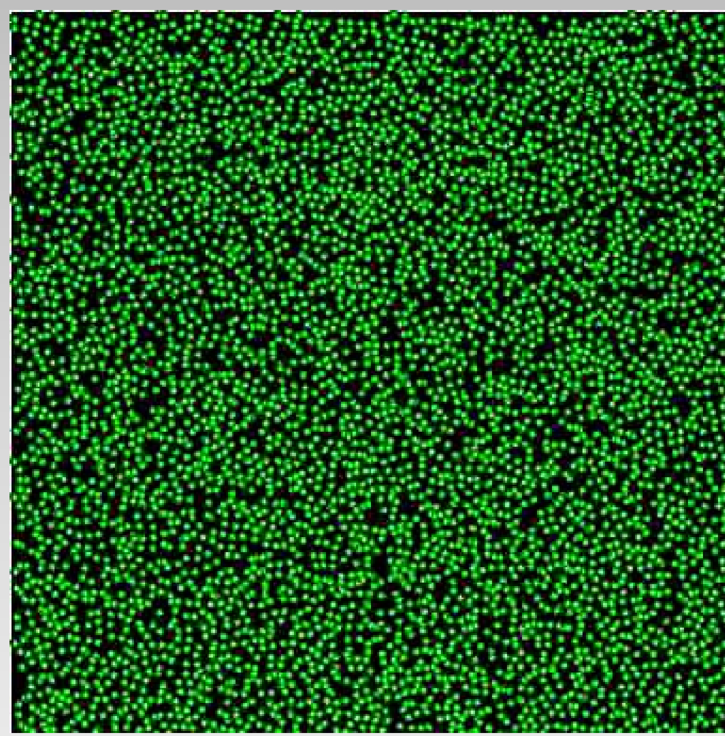

$$\phi = 0.15$$

Stability analysis

Theory:

$$\rho(x)\partial_t \mathbf{u} = -\nabla \delta p + \nu(x)\nabla^2 \mathbf{u} + \nu(x)^{-1}\mathbf{\Sigma} \cdot \nabla \nu(x) - g\delta\rho \mathbf{e}_x \quad (6)$$

$$\Sigma_{ij} = \nu(x)(\partial_i u_j + \partial_j u_i) \quad (7)$$

$$\rho(x) = \phi(x)\rho_c + (1 - \phi(x))\rho_s \quad (8)$$

$$\nu(x) = \nu_s(1 + 2.5\phi(x) + \cdots) \quad (9)$$

ansatz: $\delta\rho, \delta p \propto \exp\left(i(k_y y + k_z z) + nt\right)$ (10)

static diffusion effect: $n^*(k) = n(k) - Dk^2$ (11)

Stability analysis

Interface position: $h(y,z,t) \xrightarrow{\text{FFT}} \tilde{h}(k_y,k_z,t)$ (12)

$\langle\tilde{h}(k,t)\rangle = \langle\tilde{h}(k,0)\rangle \exp\left(n(k)t\right)$ with $k=(k_y^2+k_z^2)^{1/2}$ (13)

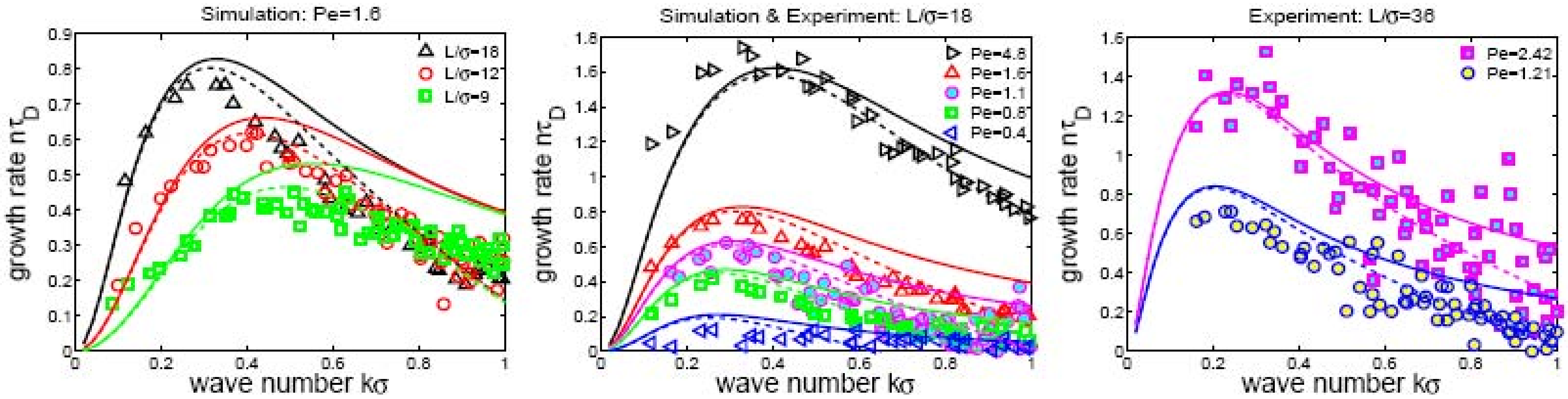

Moments of density: $\langle x \rangle$ and σ_x^2

first $\langle x \rangle$ and second moment $\sigma_x^2 = \langle x^2 \rangle - \langle x \rangle^2$ (14)

$$\langle \dots \rangle = \int_0^L \dots \phi(x,t)dx \Big/ \int_0^L \phi(x,t)dx \quad (15)$$

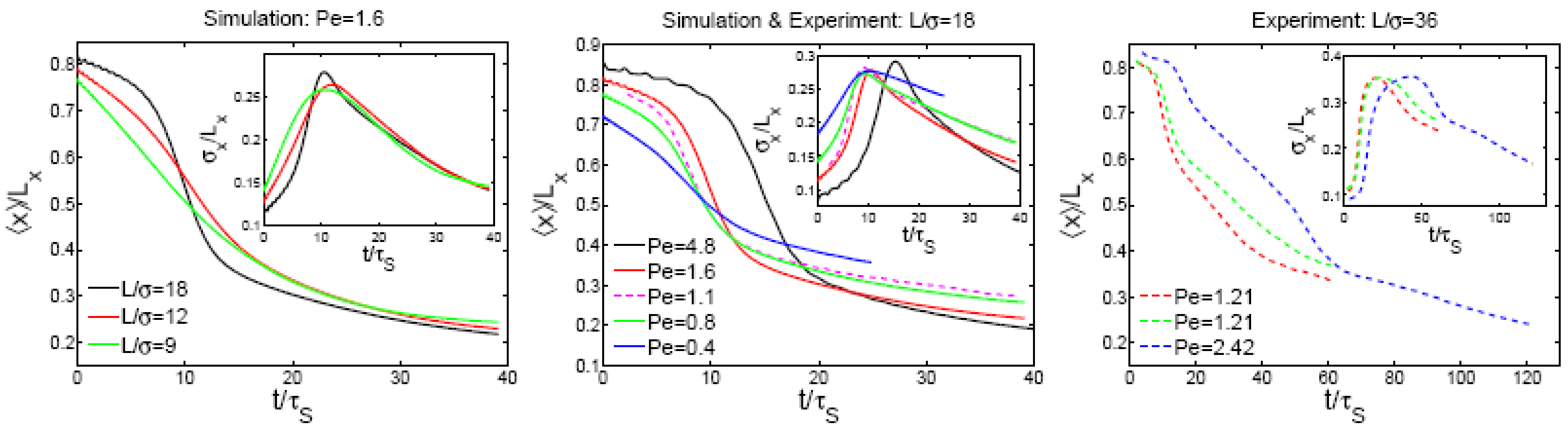

Side view of the 100 μm capillary (L/σ=36) for the Peclet number Pe=2.42.

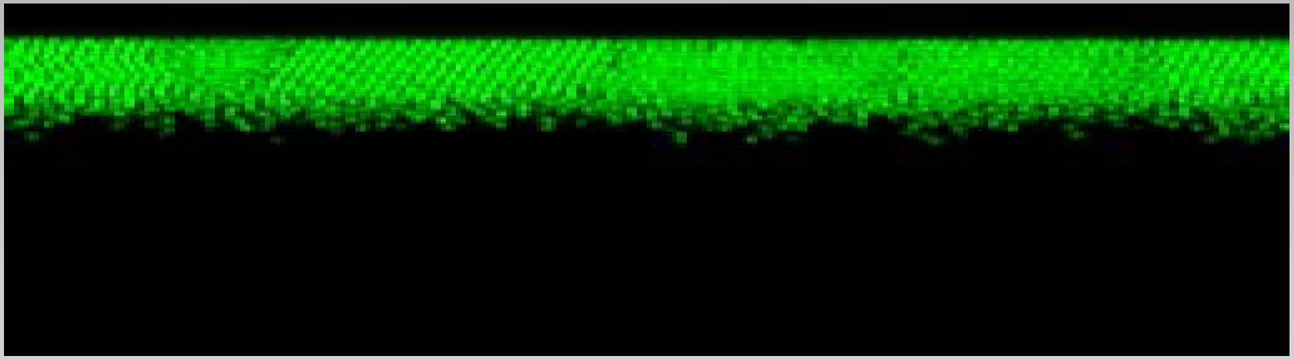

3) Lane formation in driven colloids

world's busiest pedestrian crossing

drive direction

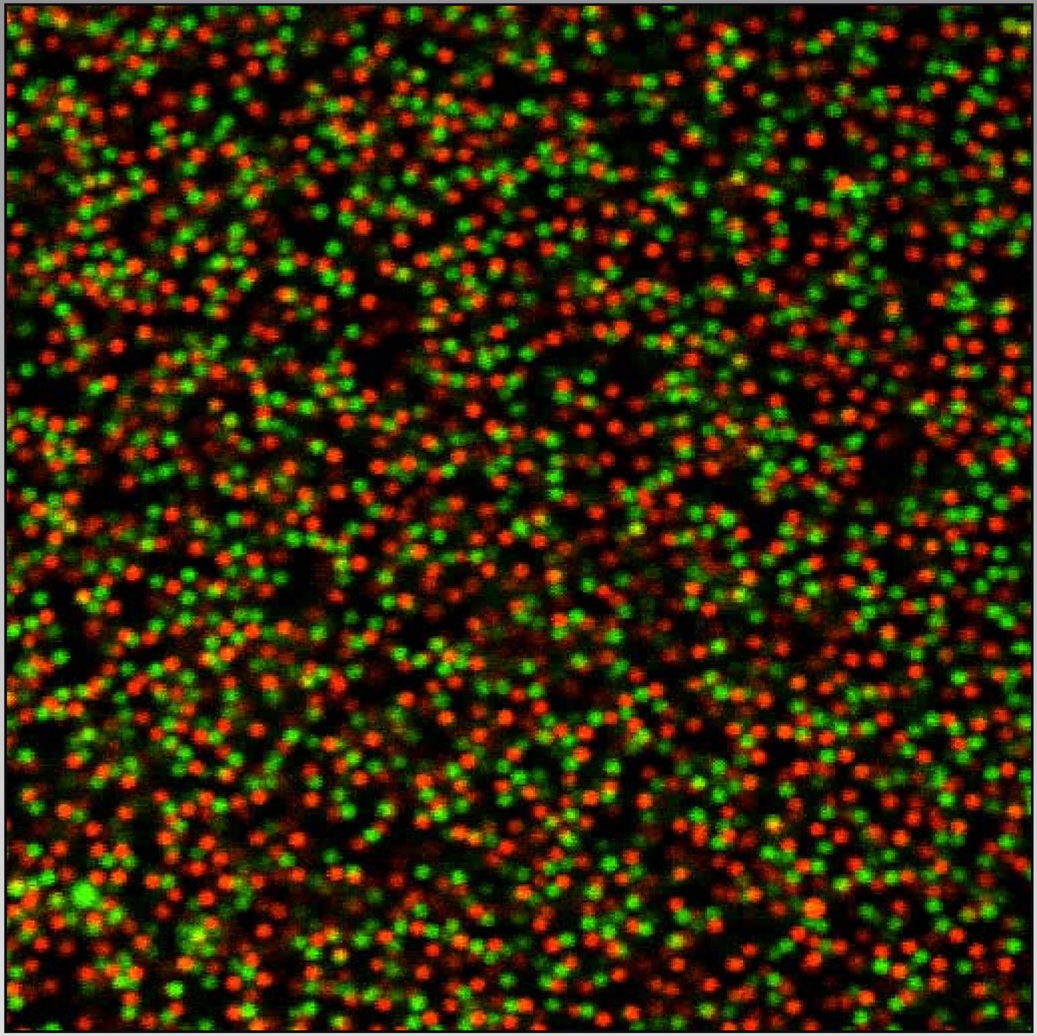

real space video by A. van Blaaderen et al.

M.E. Leunissen et al, Nature 437, 235 (2005)

I 1μ

E is continuously turned on from 0 to 50 V/mm

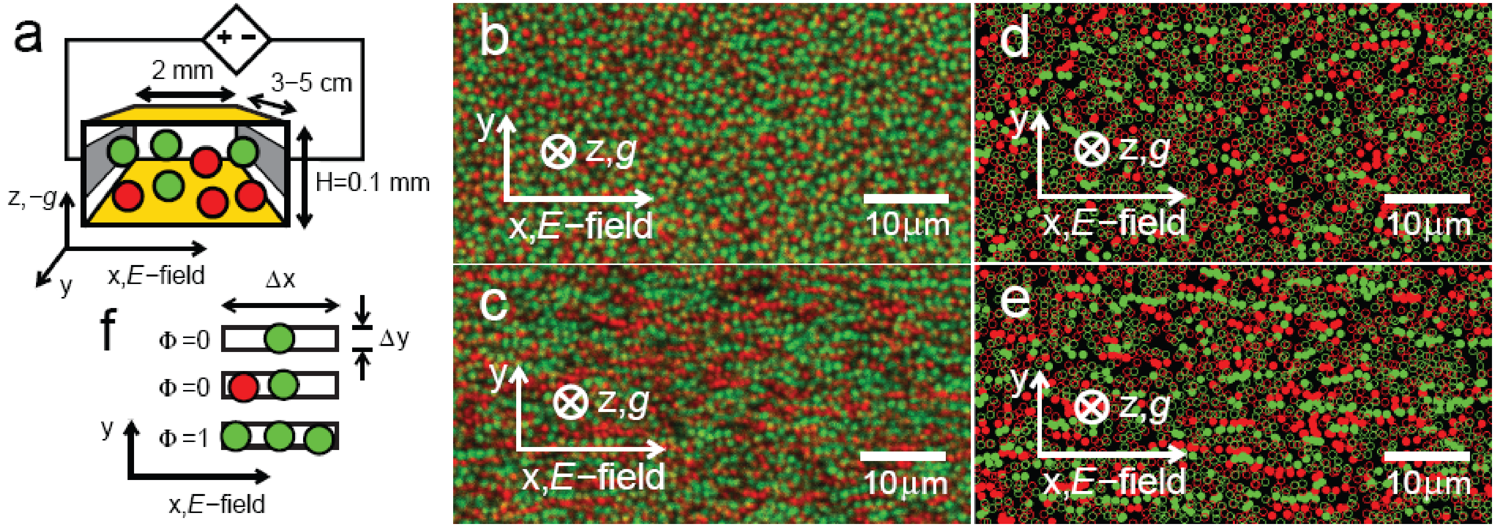

FIG. 1: **Lane formation in the experiments and simulations. a,** A sketch of the experimental setup. A suspension of oppositely charged colloidal particles is confined in a millimeter-sized capillary. A voltage is applied between electrodes. Green are negative charged NBD-labeled particles, red are positively charged RAS-labeled particles. The electric field E is directed along the **x**-axis and the gravitational field g is anti-parallel to the **z**-axis. **b-e,** Snapshots (60 μm $\times$ 30 μm) of oppositely charged particles for two different electric driving fields $E = 30$ kV/m and $E = 110$ kV/m in our experiments (b,c) and simulations (d,e). In (d,e) particles i with $\Phi_i = 1$ are depicted with filled circles and $\Phi_i = 0$ with open circles. **f,** Definition of the lane order parameter Φ. The lane order parameter for particle i is $\Phi_i = 1$ if and only if its neighbors located inside a box of dimensions $\Delta x \times \Delta y$ are of the same species.

T. Vissers, A. Wysocki, M. Rex, HL, C.P. Royall, A. Imhof, A. van Blaaderen, to be published

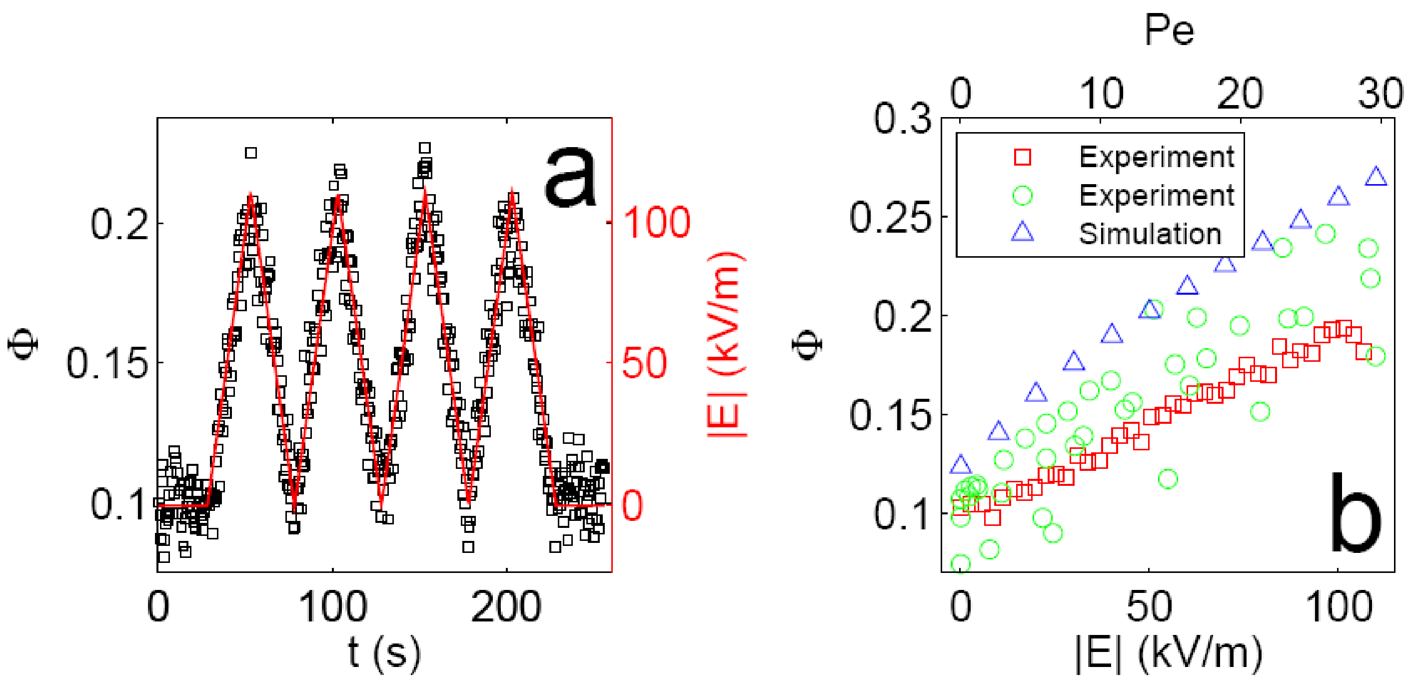

FIG. 2: **Lane order as function of field strength. a,** The time evolution of Φ with the gradually increasing and decreasing field in the experiments. The red line depicts the rise and fall of the electric field strength. **b,** The order parameter Φ as a function of the electric field strength $|E|$ for experiments in which the field was gradually changed (red squares) or applied instantaneously (green circles) and for simulations at constant field strength (blue triangles).

T. Vissers, A. Wysocki, M. Rex, HL, C.P. Royall, A. Imhof, A. van Blaaderen, to be published

influence of hydrodynamic interactions (HI)

(M. Rex, HL, EPJE 26, 143 (2008))

mobility matrix:

$$(3\pi\eta\sigma_{\mathrm{H}})\overleftrightarrow{\boldsymbol{\mu}}_{ij}$$

A) (HI) neglected:

$$\boxed{\delta_{ij}\overleftrightarrow{\mathbf{1}}}$$

B) sedimentation: Rotne-Prager (1969)

$$\delta_{ij}\overleftrightarrow{\mathbf{1}} + (1-\delta_{ij})\left[\frac{3\sigma_{\mathrm{H}}}{8}\frac{(\overleftrightarrow{\mathbf{1}} + \hat{\mathbf{r}}\otimes\hat{\mathbf{r}})}{|\mathbf{r}|} + \frac{\sigma_{\mathrm{H}}^3}{16}\underbrace{\frac{(\overleftrightarrow{\mathbf{1}} - 3\hat{\mathbf{r}}\otimes\hat{\mathbf{r}})}{|\mathbf{r}|^3}}_{\mathbb{Q}(\mathbf{r})}\right]$$

C) electrophoresis: Long Ajdari (2001)

$$\delta_{ij}\overleftrightarrow{\mathbf{1}} + \frac{3\sigma_{\mathrm{H}}}{4}(1-\delta_{ij})\left[\frac{e^{-\kappa r}}{r}\left(\left(1+\frac{1}{\kappa r}+\frac{1}{\kappa^2 r^2}\right)\overleftrightarrow{\mathbf{1}} - \left(\frac{1}{3}+\frac{1}{\kappa r}+\frac{1}{\kappa^2 r^2}\right)3\hat{\mathbf{r}}\otimes\hat{\mathbf{r}}\right) \pm \frac{1}{2}\mathbb{Q}(\mathbf{r})\right]$$

A) no hydrodynamic interactions

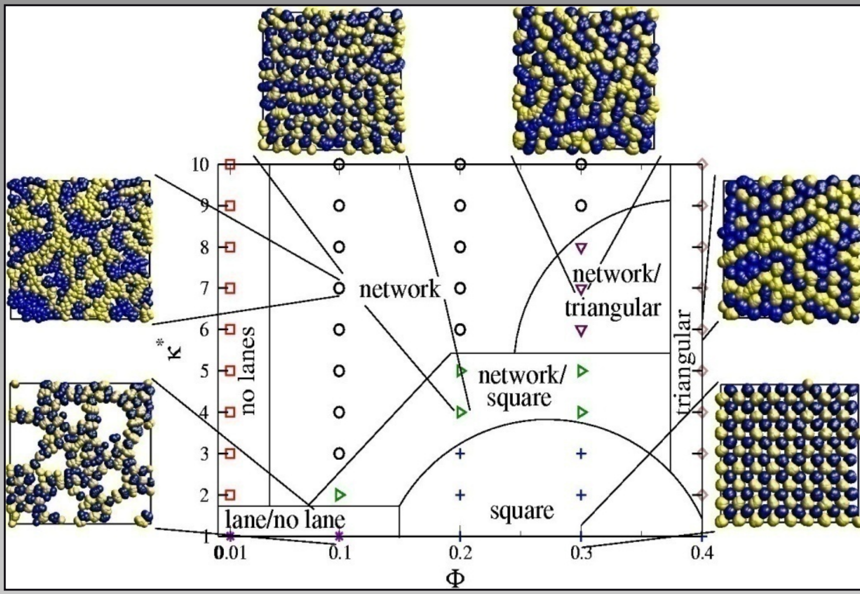

B) sedimentation: Rotne-Prager

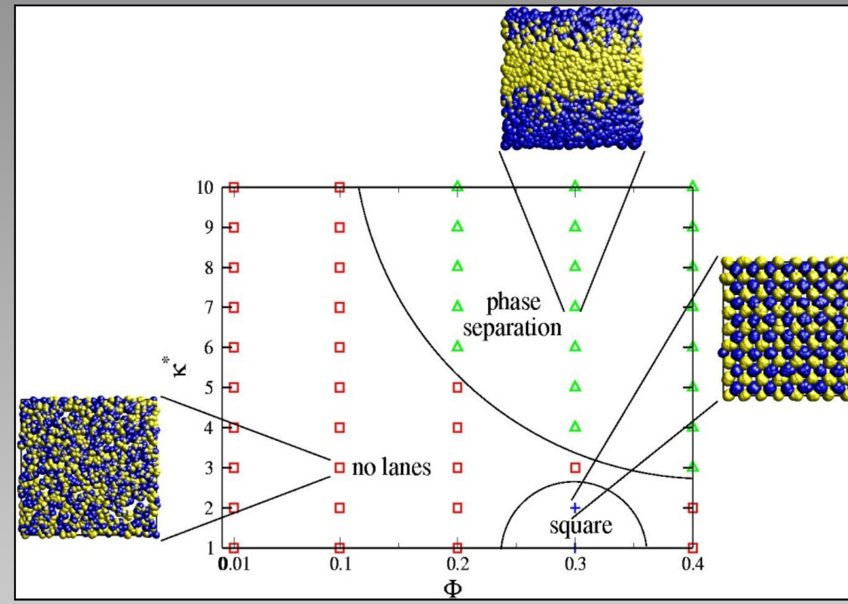

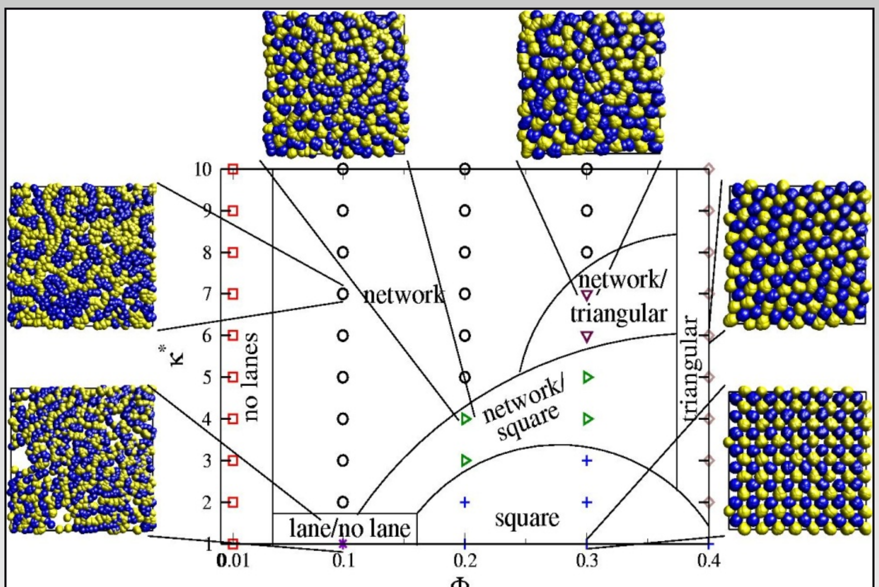

C) electric field: Long Ajdari

hysteresis for different set-ups (simulation)

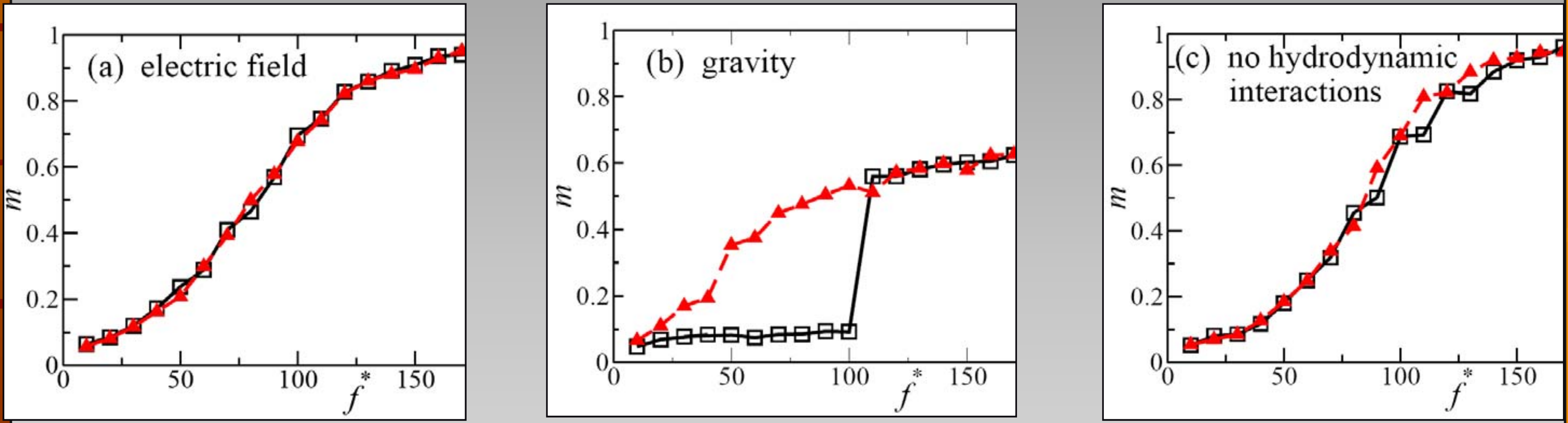

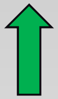

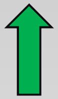

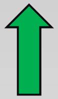

(M. Rex, PhD thesis 2008)

4) Band formation in oscillatory fields

oscillatory shaking force

$$\vec{F}(t) = \pm F_0 \sin(\omega t)\vec{e}_x$$

2d.

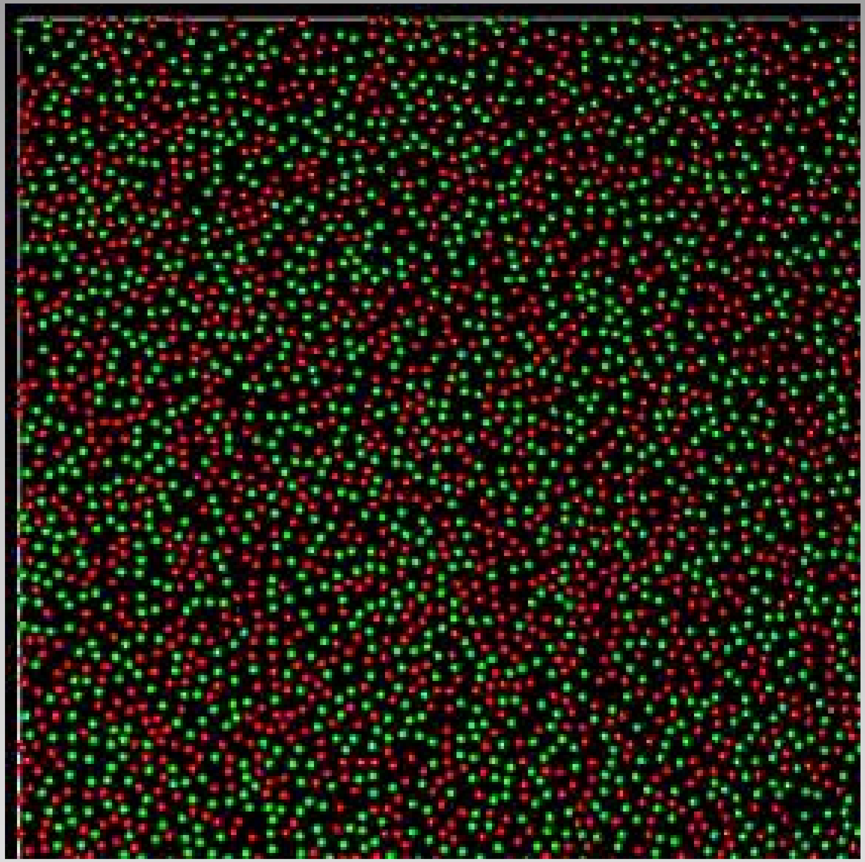

overdamped Brownian dynamics hard spheres

area fraction $\Phi = 0.4$

Peclet number

$$Pe = \frac{F_0 R}{K_B T}$$

R particle radius

A. Wysocki, HL, Phys. Rev. E **79**, 041408 2009 diffusive time scale $\tau_D = \dfrac{R^2}{D_0}$

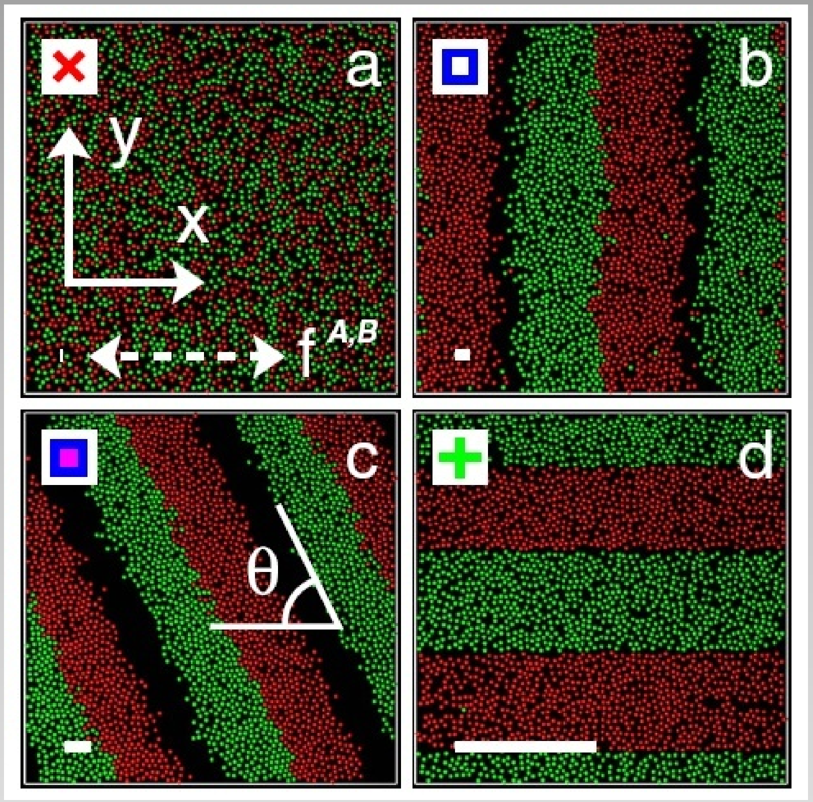

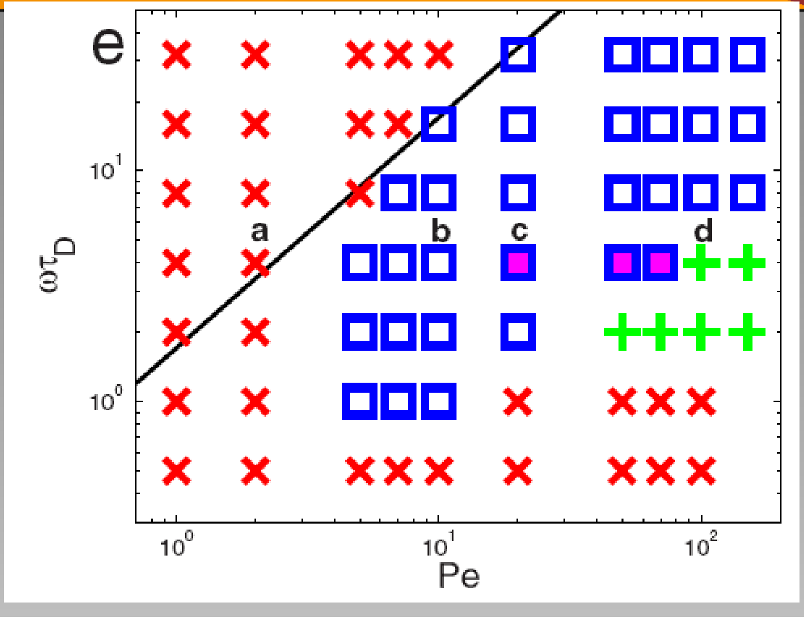

FIG. 1. (Color online) [(a)–(d)] BD simulation snapshots for fixed driving frequency $\omega\tau_D$=4 but different Peclet numbers Pe after 10^4 periods starting from a fully mixed configuration. Particles colored in green (light gray) are of species A while particles colored in red (dark gray) are of species B. Symbols in the left upper corner correspond to symbols used in (e). In (a) the coordinate frame is shown and the direction of the driving field is indicated by the broken arrow. In (a)–(d) the length of the solid bars (bottom left corner) correspond to the amplitude of a free particle driven without noise in the external field. For small Pe, we observe a disordered state (a), for intermediate Pe colloids segregate into stripes oriented perpendicular or tilted (tilt angle θ) to the direction of the oscillating force [(b)–(c)], on the other hand, for high Pe, lanes are formed parallel to the direction of the oscillatory force (d). Parameters are $\omega\tau_D$=4 and Pe=2,10,20,110 from (a) to (d). (e) Nonequilibrium steady-state phase diagram for fixed area fraction ϕ=0.4. The solid line describes the simple theoretical estimate of the disordered-to-segregated phase boundary.

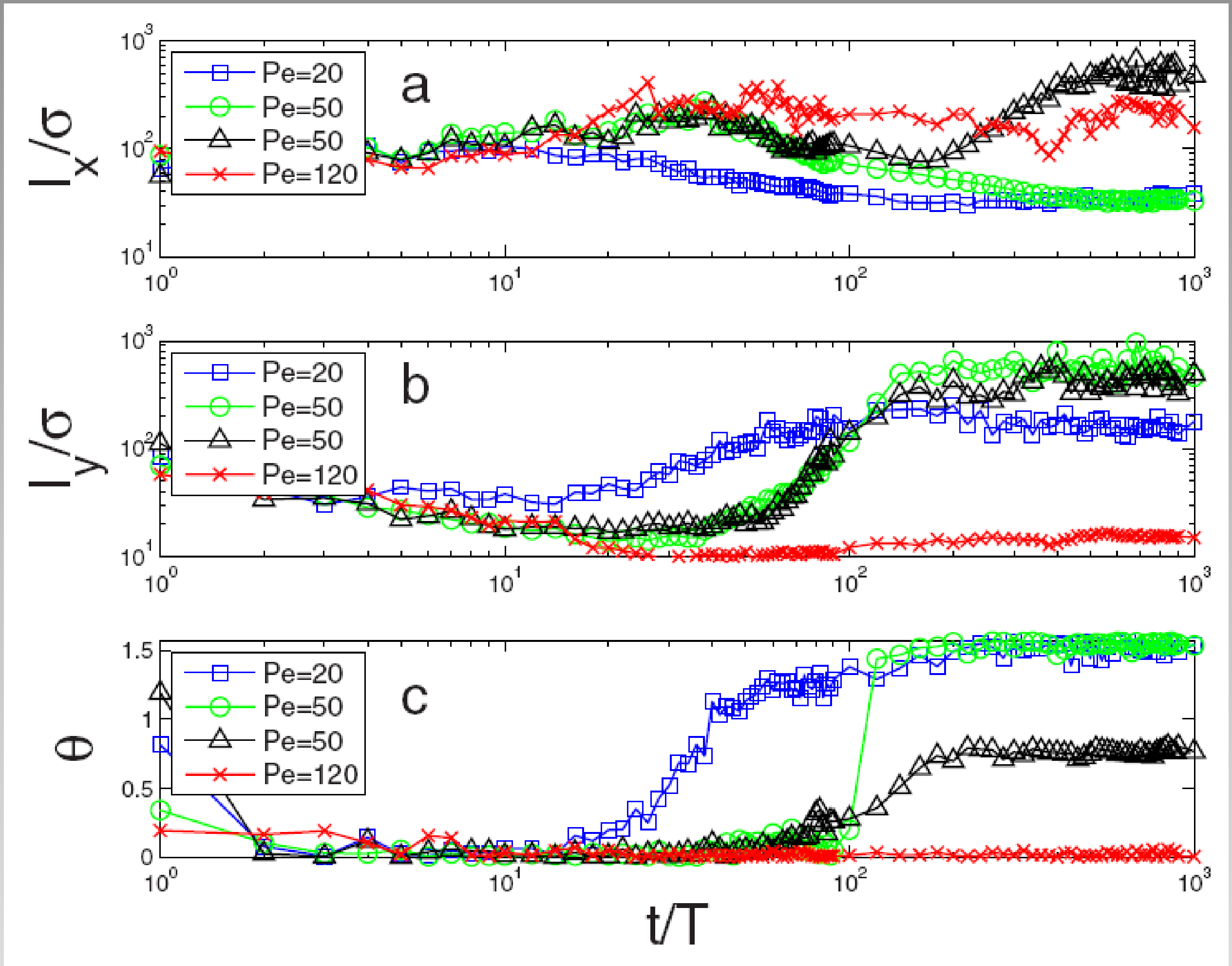

FIG. 2. (Color online) Time evolution of a typical length scale (a) l_x/σ parallel and (b) l_y/σ perpendicular to the direction of the oscillatory force, (c) as well as of the orientation θ of a typical structure. The angular frequency is fixed $\omega\tau_D=4$. For Pe=20 the system end in an axial segregated state (blue square), for Pe=50 both segregated (green circle) and tilted (black triangle) states occur, whereas for Pe=120 the steady state is laning (red cross).

$$\boxed{\sigma = 2R}$$

MPCD simulations (in 2d) in order to explore the influence of hydrodynamic interactions on banding

(Adam Wysocki, HL, to be published)

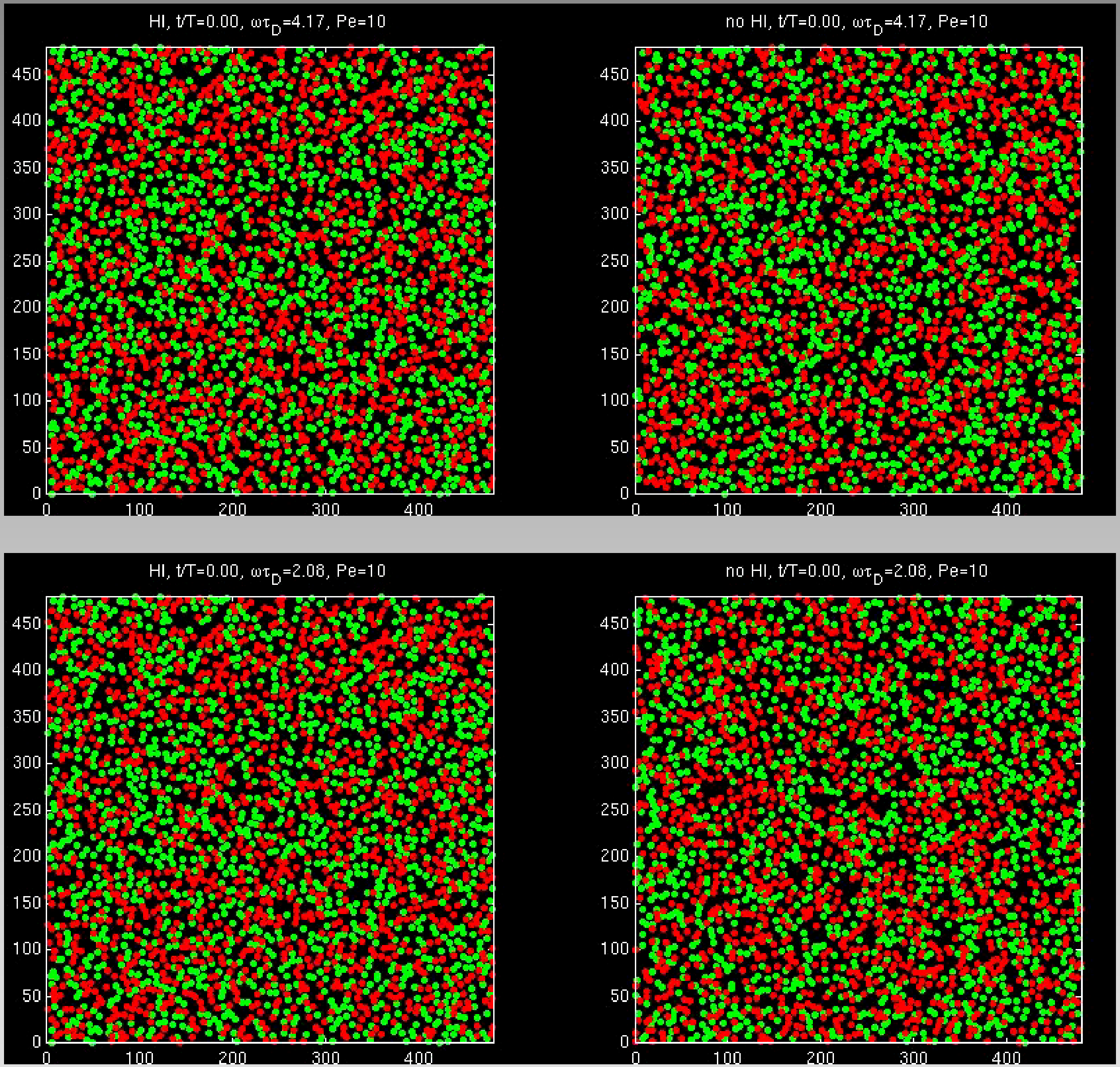

HI destroy banding … and lead to new bands …

intermittency!?

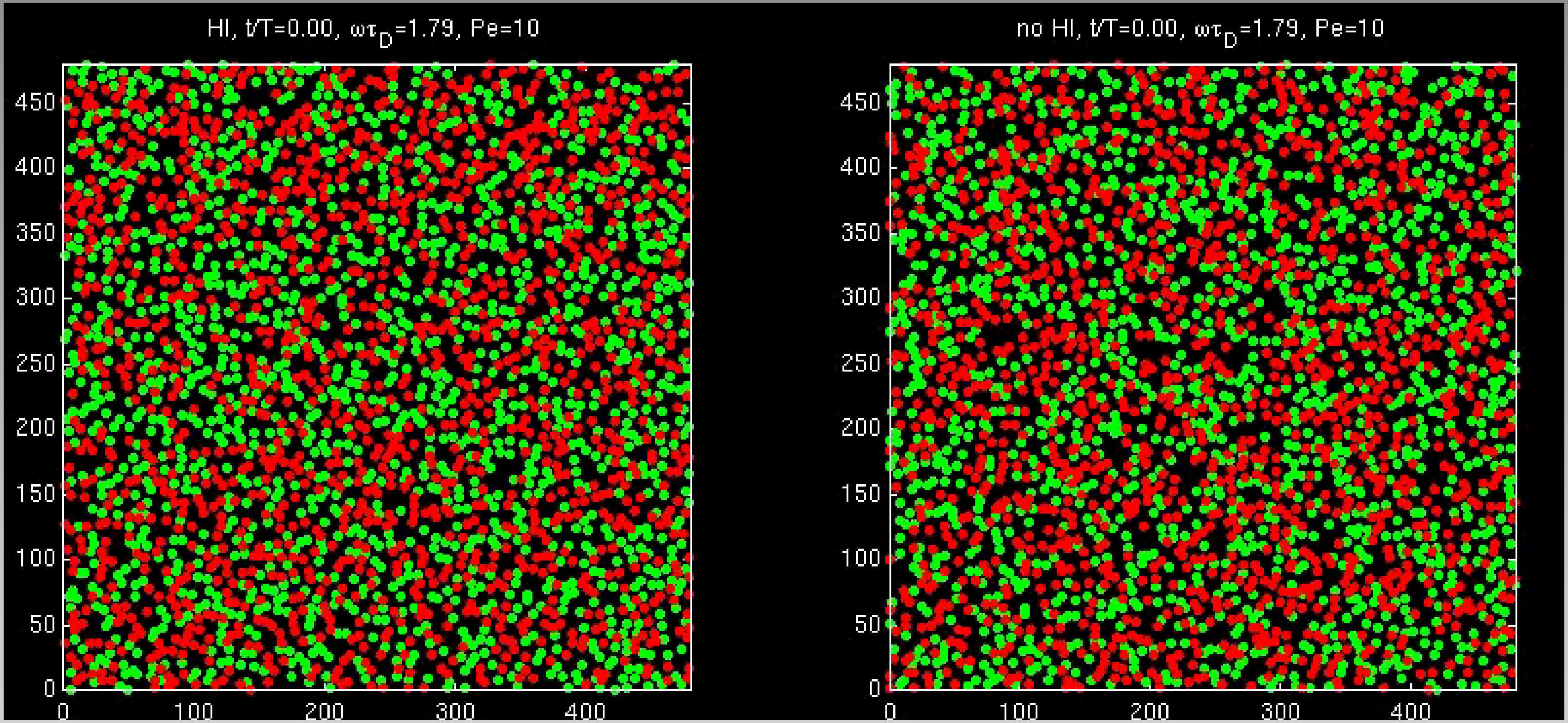

HI, t/T=0.00, ωτ_D=1.79, Pe=10
no HI, t/T=0.00, ωτ_D=1.79, Pe=10
0
50
100
150
200
250
300
350
400
450
0
100
200
300
400

enstrophy $\mathcal{S} = \frac{1}{2}\int_A |\nabla \times \mathbf{v}|^2 \, d^2\mathbf{r}$

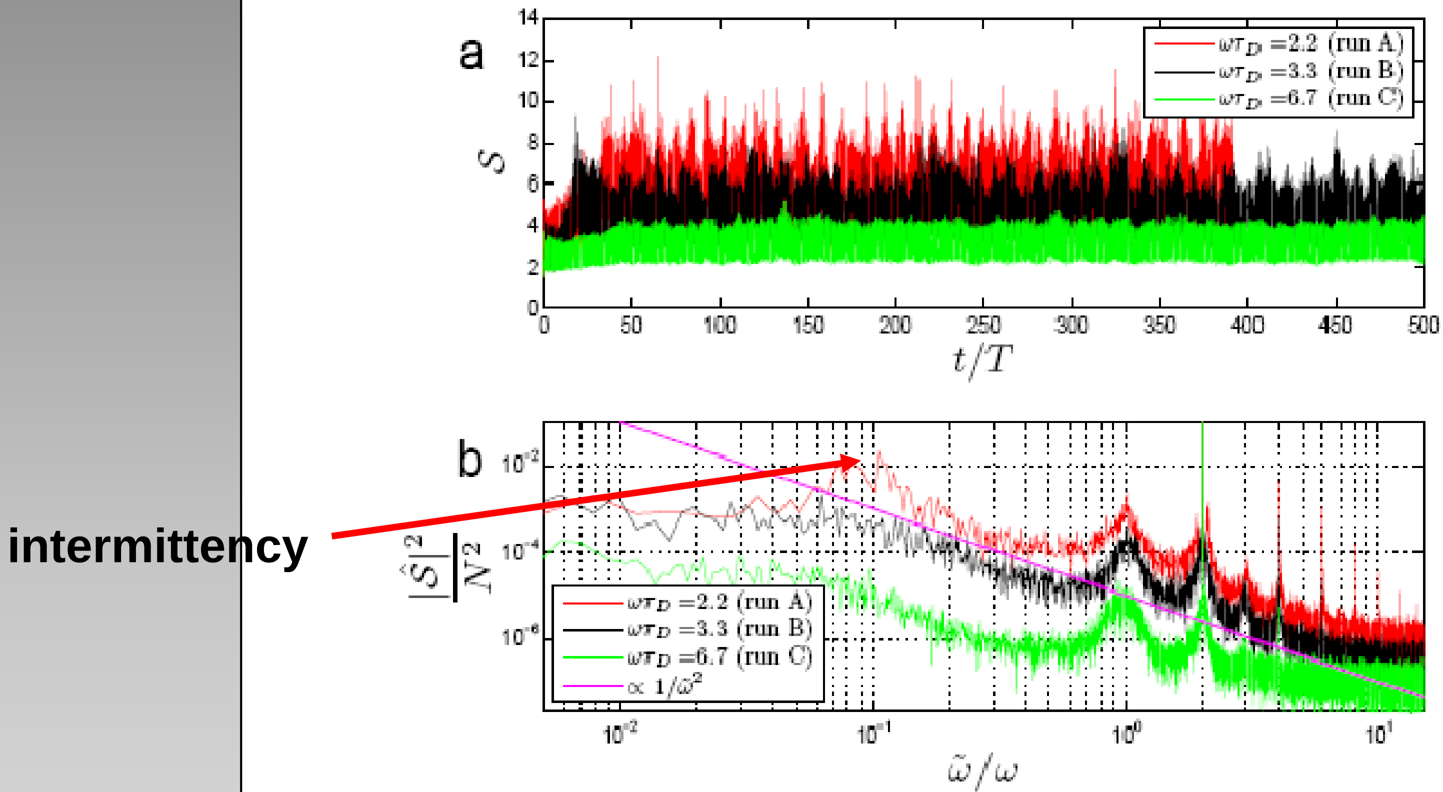

Figure 4. (a) Time dependence of the enstrophy $\mathcal{S} = \frac{1}{2}\int_A |\nabla \times \mathbf{v}|^2 \, d^2\mathbf{r}$ belonging to the solvent velocity field $\mathbf{v}(\mathbf{r})$ for run A, B and C. Time is normalised by corresponding driving period $T = 2\pi/\omega$. (b) Log-log plot of the power spectrum $\frac{|\hat{\mathcal{S}}|^2}{N^2}$ of the enstrophy $\mathcal{S}$ versus the frequency $\tilde{\omega}$. $\hat{\mathcal{S}}(\tilde{\omega})$ is the Fourier transformed of $\mathcal{S}$ and $\tilde{\omega}$ is normalised by the corresponding driving frequency ω. The dashed line indicate an inverse quadratic scaling of the spectrum, i.e. $|\hat{\mathcal{S}}|^2 \propto \tilde{\omega}^2$.

Video A. van Blaaderen

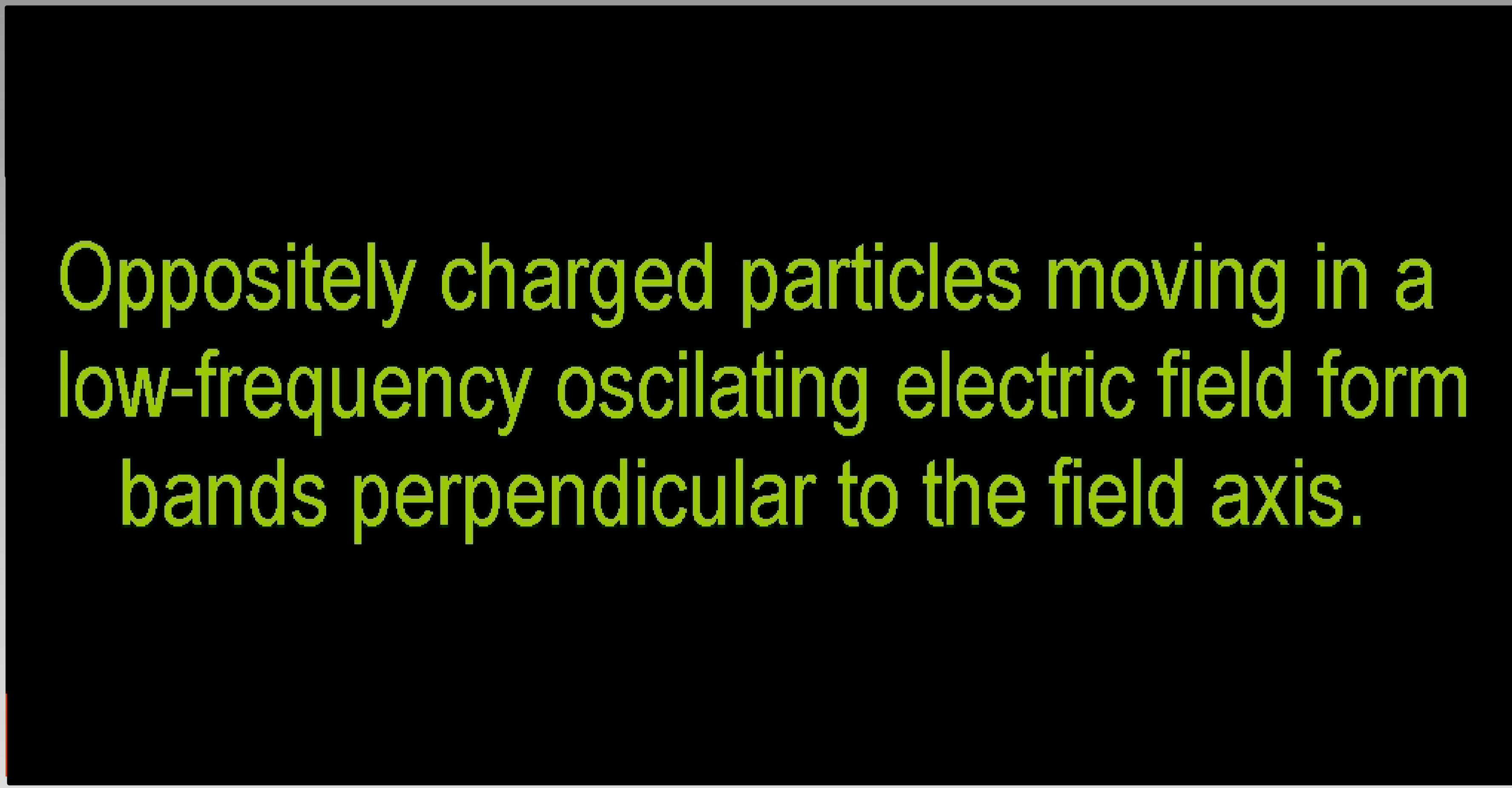

$\vec{E}$

comparison with BD simulations of Yukawa mixture is in progress

5) Lane formation in complex plasmas

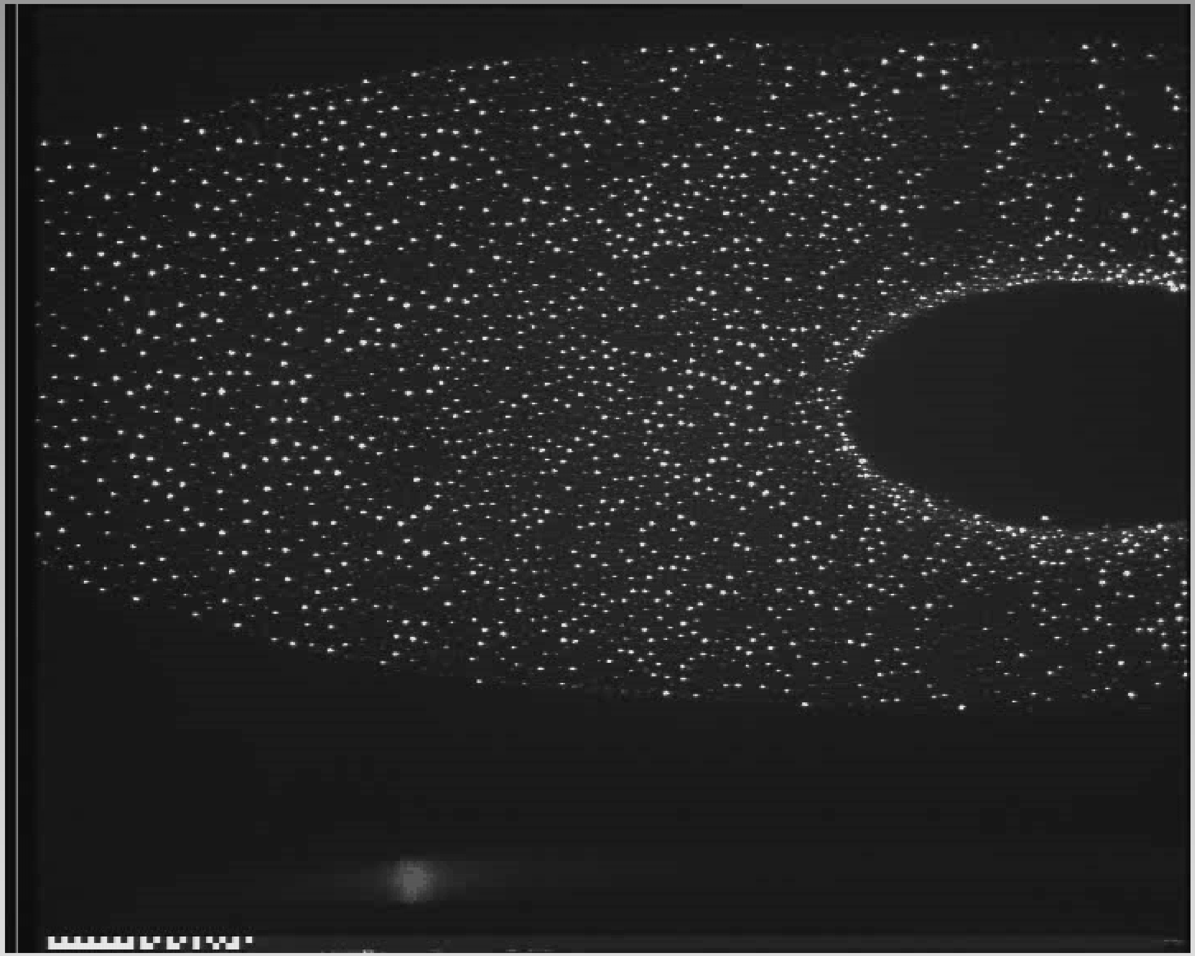

laning: K. R. Sütterlin et al, Phys. Rev. Letters 102, 085003 (2009)
kinetics of demixing: A. Wysocki et al, Phys. Rev. Letters 105, 045001 (2010)

Lane formation (simulation)

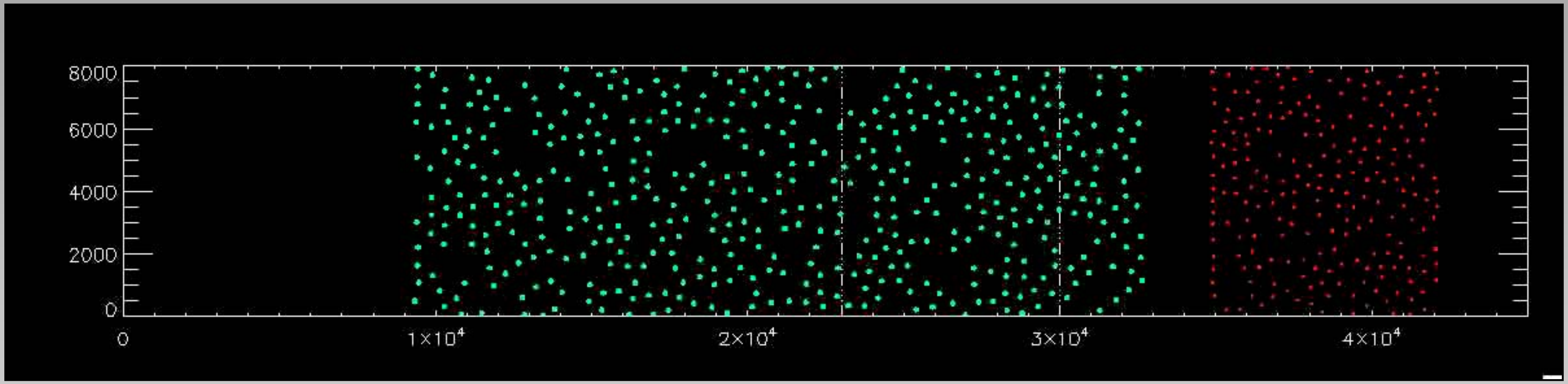

binary Yukawa system with damped molecular dynamics

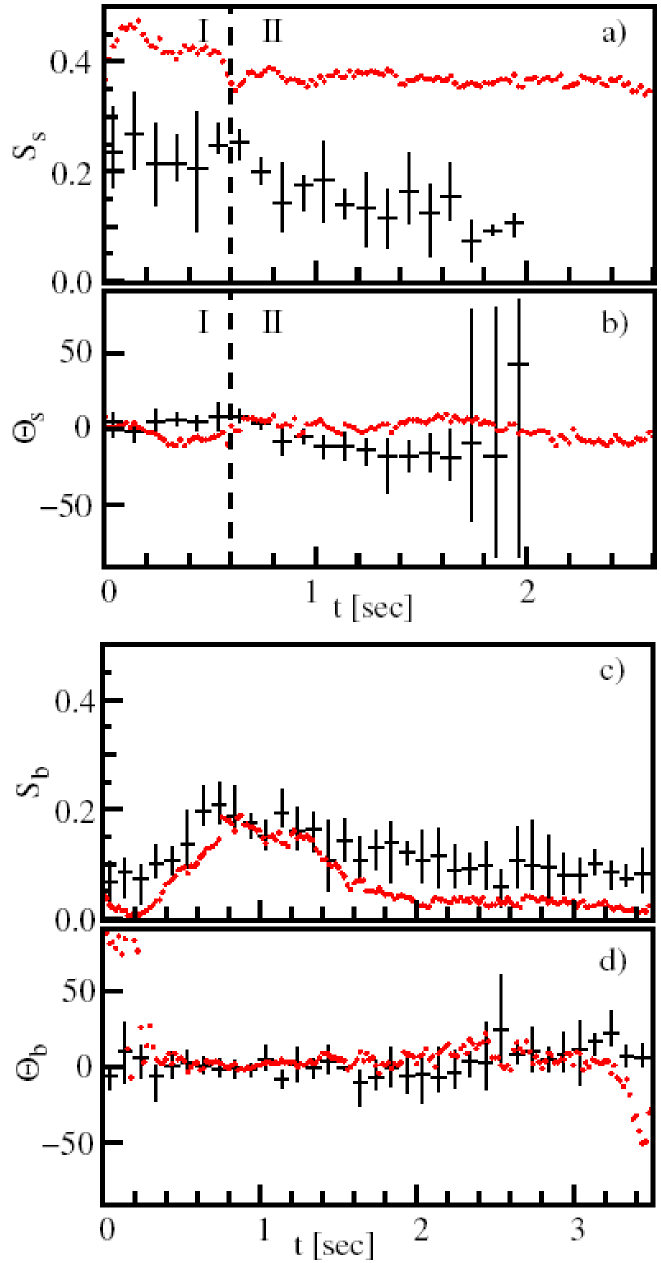

Dynamics of laning. Shown are the evolution of the "nematic" order parameter for small and big particles, S_s (a) and S_b (c), respectively, as well as the corresponding global laning angle, Θ_s (b) and Θ_b (d), as obtained from the anisotropic scaling index analysis of the experiment (crosses) and MD simulation (dots). For small particles, injection stage I and steady-state stage II are indicated.

6) Conclusions

Colloidal dispersions in time-dependent external fields are excellent model systems for nonequilibrium phenomena on the particle scale.